Cerebral Cortex November 2012;22:2478–2485
doi:10.1093/cercor/bhr327
Advance Access publication November 22, 2011

# Longitudinal Development of Cortical and Subcortical Gray Matter from Birth to 2 Years

John H. Gilmore[1,2], Feng Shi[2,3], Sandra L. Woolson[1], Rebecca C. Knickmeyer[1], Sarah J. Short[1], Weili Lin[2,3], Hongtu Zhu[2,4], Robert M. Hamer[1,4], Martin Styner[1,5] and Dinggang Shen[2,3]

[1]Department of Psychiatry, [2]Biomedical Research Imaging Center, [3]Department of Radiology, [4]Department of Biostatistics and [5]Department of Computer Science, University of North Carolina at Chapel Hill, Chapel Hill, NC 27599-7160, USA

Address correspondence to John H. Gilmore, Department of Psychiatry, 10522 Neurosciences Hospital, CB# 7160, UNC School of Medicine, Chapel Hill, NC, 27599-7160. Email: jgilmore@med.unc.edu.



**Very little is known about cortical development in the first years of life, a time of rapid cognitive development and risk for neurodevelopmental disorders. We studied regional cortical and subcortical gray matter volume growth in a group of 72 children who underwent magnetic resonance scanning after birth and at ages 1 and 2 years using a novel longitudinal registration/parcellation approach. Overall, cortical gray matter volumes increased substantially (106%) in the first year of life and less so in the second year (18%). We found marked regional differences in developmental rates, with primary motor and sensory cortices growing slower in the first year of life with association cortices growing more rapidly. In the second year of life, primary sensory regions continued to grow more slowly, while frontal and parietal regions developed relatively more quickly. The hippocampus grew less than other subcortical structures such as the amygdala and thalamus in the first year of life. It is likely that these patterns of regional gray matter growth reflect maturation and development of underlying function, as they are consistent with cognitive and functional development in the first years of life.**

**Keywords:** amygdala, cerebral cortex, hippocampus, lateral ventricle, magnetic resonace imaging

## Introduction

The first 2 years of life are the most dynamic and perhaps the most critical phase of postnatal brain development. Concurrent with the rapid pace of structural brain growth is an equally rapid development of a wide range of cognitive and motor functions (Kagan and Herschkowitz 2005). Abnormalities in early postnatal brain development have been implicated in neurodevelopmental disorders, including enlarged lateral ventricles and increased cortical gray matter volumes in infant males at genetic high risk for schizophrenia (Gilmore, Kang, et al. 2010), and "overgrowth" of gray matter volumes in the first year of life in children who go on to develop autism (Hazlett et al. 2005; Courchesne et al. 2007; Amaral et al. 2008). In spite of its importance for understanding normal brain development and the early origins of neurodevelopmental disorders, our knowledge of human brain development in this crucial time period is not well developed. While there has been great interest in magnetic resonance imaging (MRI) studies of normal human brain development, most studies to date have not included the first years of life (Giedd et al. 1999; Sowell et al. 1999; Sowell et al. 2003; Gogtay et al. 2004; Sowell et al. 2004; Shaw et al. 2008).

While cortical gyrification and folding at birth is very similar to that observed in adults (Chi et al. 1977; Hill et al. 2010), there is an enormous growth of gray matter volume in the first years of life (Matsuzawa et al. 2001). We have previously found that cortical gray matter volume increases by 149% in the first year of life and by 14% in the second (Knickmeyer et al. 2008). This rapid growth of gray matter volume is consistent with postmortem studies indicating rapid development of synapses and spines during this time period (Huttenlocher and Dabholkar 1997; Glantz et al. 2007; Petanjek et al. 2011; Webster et al. 2011) and coincides with rapid maturation of white matter in this time period (Yakovlev and Lecours 1967). In the neonatal period, we found a posterior to anterior gradient of gray matter growth (Gilmore et al. 2007) consistent with regional differences in cortical synapse development that has been described in human brain (Huttenlocher and Dabholkar 1997).

There is clear evidence of regional differences in the developmental trajectories of cortical gray matter maturation in older children and adolescents, thought to reflect differences in the development of earlier maturing sensory and motor functions versus later maturing higher-order integrative functions (Sowell et al. 2003; Gogtay et al. 2004; Sowell et al. 2004; Shaw et al. 2008). In contrast, very little is known about gray matter development in early childhood. Nonuniform differential rates of cortical expansion were observed in a small group of infants compared with adults, with regions of lateral temporal, parietal, and frontal cortex expanding almost twice as much as occipital, medial temporal, and insular cortex (Hill et al. 2010). Our previous study (Knickmeyer et al. 2008) evaluated overall cortical gray matter development with a cross sectional design but was not able to delineate longitudinal development in more precise cortical regions. Here, we applied a novel longitudinal registration method that allows comparison of neonatal scans to those of 1 and 2 years olds, across a period of rapid volume expansion, changing tissue contrasts, and rapid myelination.

## Materials and Methods

This study was approved by the Institutional Review Board of the University of North Carolina at Chapel Hill. Subjects were part of a large prospective study of early brain development in healthy singleton and twin children (Gilmore et al. 2007, Knickmeyer et al. 2008; Gilmore, Schmitt, et al. 2010). Subjects were recruited prenatally and scanned shortly after birth, and at ages 1 and 2 years; representative scans are presented in Figure 1. Children were also assessed with the Mullen Scales of Early Learning (Mullen 1995) at ages 1 and 2 years. Children with successful scans at each time point were screened for this study; exclusion criteria were 1) gestational age at birth less than 32 weeks, 2) stay in the neonatal intensive care unit for more than 1 day, 3) abnormality on MRI other than a minor intracranial hemorrhage, common in the neonatal period (Looney et al. 2007), 4) Mullen composite score at age 1 or 2 years less than 71, and 5) major medical or neurologic illness after birth. Seventy-three children were identified and included in this analysis.

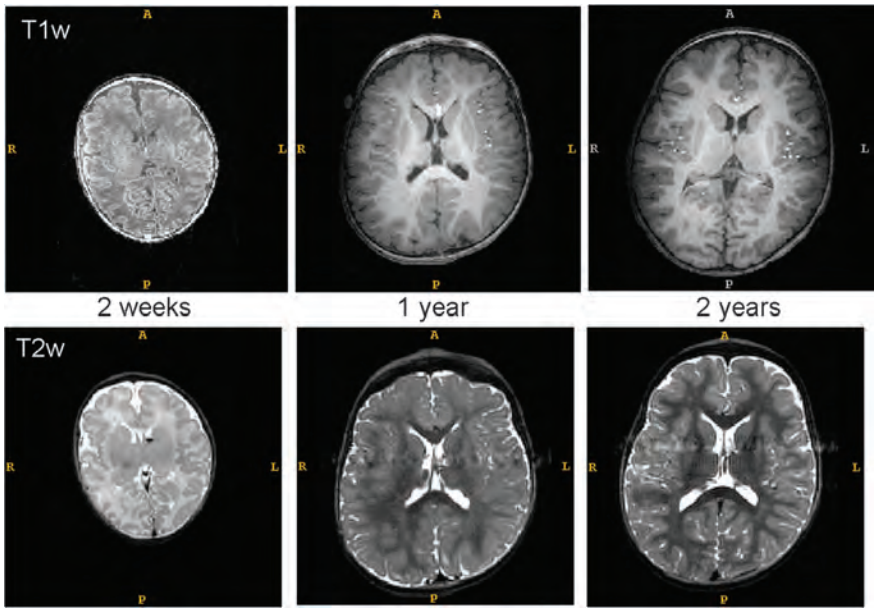


**Figure 1.** Representative longitudinal $T_1$ and $T_2$ weighted scans in a neonate, 1 and 2 year old.

### *Image Acquisition*

Images were acquired on a Siemens head-only 3T scanner (Allegra, Siemens Medical System, Erlangen, Germany). Children were scanned unsedated while asleep, fitted with ear protection and with their heads secured in a vacuum-fixation device. $T_1$-weighted structural pulse sequences were a 3D magnetization prepared rapid gradient echo (MP-RAGE time repetition [TR] = 1820 ms, inversion time = 1100 ms, echo time = 4.38 ms, flip angle = 7°, and $n$ = 144). Proton density and $T_2$-weighted images were obtained with a turbo spin echo sequence (TR = 6200 ms, time echo [TE]1 = 20 ms, TE2 = 119 ms, and flip angle 150°). Spatial resolution was 1 × 1 × 1 mm voxel for $T_1$-weighted images, 1.25 × 1.25 × 1.5 mm voxel with 0.5-mm interslice gap for proton density/$T_2$-weight images. For children who failed or were deemed likely to fail due to difficulty sleeping, a "fast" sequence was done; 12 neonates had a "fast" $T_2$ scan with a decreased TR, image matrix and number of slices (5270 ms, 104 × 256 mm, 50) and 3 one year olds had a "fast" T1 scan with a decreased image matrix (144 × 256 mm).

### *Image Analysis*

We applied a novel 4D longitudinal warping approach (Shi et al. 2011) for segmentation and 90 region parcellation that involved 1) the intensity-based segmentation of the 2-year-old brain image and the creation of a subject-specific tissue probabilistic atlas, and 2) probabilistic atlas based tissue segmentation on the images acquired at 2-week old and 1-year old according to the warped tissue probabilistic atlas of 2-year old using a simultaneous registration and segmentation framework. $T_1$ images were used for 1 and 2 year olds and $T_2$ images for neonates.

Tissue segmentation of 2-year-old brain was performed after intensity inhomogeneity correction using an adaptive fuzzy c-means automatic brain tissue segmentation method (Pham and Prince 1999). The resulting tissue probabilistic maps of gray matter (GM), white matter (WM), and cerebrospinal fluid (CSF) were used as subject-specific tissue probabilistic atlases for guiding the segmentation of the 2-week-old and 1-year-old images of the same subject, since cortical convolution patterns of the same subject remain similar after normal birth (Chi et al. 1977; Hill et al. 2010). Because the subject-specific tissue probabilistic maps exhibit considerably smaller anatomical variability compared with cross-sectional maps, they are able to provide more precise and longitudinally consistent segmentation results. A joint registration and segmentation framework was used to progressively refine in an iterated fashion 1) the registration of the 2-year-old image with 2-week-old and 1-year-old images, respectively, and 2) the atlas-based segmentation of 2-week-old and 1-year-old images (Shi et al. 2010). All registrations are performed on the segmented images, thus the dynamic GM/WM contrast changes from 2-week old to 2-year old do not affect the registration performance. This 4D tissue segmentation and registration algorithm has been validated by comparing with the manual segmentations and shows very good performance (Shi et al. 2011).

Based on this 4D segmentation and registration algorithm, we labeled the whole brain into 90 regions at each age, by using the 90-regions atlas provided by Tzourio-Mazoyer et al. (2002). Specifically, the 2-year-old image is first parcellated with the 90-regions atlas by warping it onto the 2-year-old image space using the HAMMER registration algorithm (Shen and Davatzikos 2002). The parcellation result is then propagated onto the 1-year-old and the neonate images sequentially by using the longitudinal correspondences established among images of 3 ages by the 4D segmentation and registration algorithm (Shi et al. 2011).

To validate the parcellation results, 3 regions (left superior frontal gyrus, left hippocampus, and right middle temporal gyrus) were manually segmented by 3 raters on 5 subjects at each age, that is, 2-week old, 1-year old, and 2-year old. Leave-one-out (LOO) cross validation was used to evaluate the performance of our brain labeling method; in each LOO case, images of 4 subjects were first nonlinearly aligned by HAMMER (Shen and Davatzikos 2002) to build the label atlases for the 3 respective labels. Then, for the left-out subject, the built label atlases are warped onto different age images of this left-out subject. Thus, the warped labels can be compared with the 3 manual-labeled brain structures of this left-out subject, to measure the respective overlap rates by the Dice coefficient (Dice 1945). The results on all 5 LOO cases show that the average overlap rate between the automated and the manual labeling results is around 0.7, which is comparable to the average interrater overlap rate. This validation experiment indicates that our brain labeling method has comparable accuracy with manual raters.

Total volume is reported for the subcortical structures as intermediate intensity values, for gray and white matter in these structures did not allow precise tissue segmentation. The volume of the lateral ventricles was segmented with a user-initialized semiautomatic surface evolution from the CSF tissue probability map using a level-set evolution tool kit, itk-SNAP (http://itksnap.org/download/snap/).

### *Statistical Analysis*

All statistical analyses were performed using SAS statistical software, version 9.2. For demographic variables, frequency distributions were

calculated for categorical variables and means (standard deviations [SD]) were calculated for continuous variables. The means (SD) were also calculated for the 90 brain regions of interest. Mixed models were used to calculate the least-squares means for years 0, 1, and 2, and corresponding percent changes for years 1 and 2. The study sample included both singletons and twins, so mixed models methodology was used to treat the twins as replications, while the singletons had no replicates. Because the data were longitudinal, an autoregressive covariance structure was used. The mixed models included baseline total gray matter, gender, year of MRI, twin status, gender by year of MRI interaction, and twin status by year of MRI interaction. All statistical hypothesis tests were two-tailed and conducted at a significance level of 0.05. There were no adjustments made for multiple comparisons; for this reason, and because number of regions studies exceeded the number of subjects, the results should be considered descriptive and hypothesis generating.

## Results

The final sample of 73 subjects consisted of 30 singletons (20 males/10 females) and 43 twins (22 males/21 females; 7 monozygotic twin pairs, 10 dizygotic pairs, 8 "single" twins). Ethnic composition was 49 Caucasian, 23 African-American, and 1 Asian-American. Mean gestational age at birth was 37.9 ± 1.6 weeks (mean ± SD); mean birth weight was 2.93 ± 0.56 kg. Mean age at the neonatal scan: 25.5 ± 10.8 days; at year 1: 1 year, 27.8 ± 22.1 days; at year 2: 2 years, 28 ± 38.1 days.

Table 1 presents cortical gray matter volumes at each age, as well as percent growth rate over time in each region. Table 2 presents similar information for subcortical structures. Figures 2 and 3 present a surface rendering of relative growth rates by cortical region for the first and second years of life, respectively.

### *Gray Matter Growth Year 1*

Total cortical gray matter increased 108% in the first year. There was variation across cortical regions in growth rates, ranging from 62% to 154%. Interestingly, the regions with the slowest growth rates were sensory/motor regions, including the postcentral gyrus, paracentral lobule, Heschl gyrus, cuneus, and cortex surrounding the calcarine fissure, as well as the superior temporal gyrus. Faster growing regions in the first year included the insula, inferior frontal gyrus (opercular part), superior frontal gyrus (orbital part), inferior temporal gyrus, temporal pole of the middle temporal gyrus, median cingulate and paracingualte gyri, angular gyrus, and the fusifom gyrus.

### *Gray Matter Growth Year 2*

Total cortical gray matter increases about 19% in the second year of life, with a range of 9–28%. Slower growing regions include the slower growing regions of the first year: postcentral gyrus, calcarine, paracentral lobule, as well as other regions: Rolandic operculum, gyrus rectus, posterior cingulate gyrus, and the middle and inferior occipital gyri. Faster growing regions were identified in the parietal lobe: inferior, angular, and supramarginal gyri; the frontal lobe: dorsolateral and medial superior frontal gyri, middle frontal gyrus; as well as the temporal pole of the middle temporal gyrus.

### *Subcortical Structures*

Total volume of the subcortical structures increased at a similar rate between 104% and 107% in the first year of life, except for the hippocampus, which grew at a slower rate of 82–86%. In the second year, there was more variability in the growth rates, with the smallest volume increases in the putamen and the largest increases in the palladium and hippocampus.

While this study was not adequately powered to definitively address these questions, we explored the effect of gender and twin/singleton status on growth rates. While males consistently had larger regional gray matter volumes than females, males and females had similar growth rates in all but 9 regions after correcting for multiple comparisons. We have previously found neonatal brain structure to be similar between twins and singletons (Knickmeyer et al. 2011). In this study, we found twins and singletons had similar growth rates in all but 4 regions.

## Discussion

This is the first study of regional cortical gray matter volume maturation in the first years of life using a longitudinal sample. Our results show that cortical regions have distinct maturational trajectories. Overall cortical gray matter volume growth is rapid, with volume increasing 108% in the first year of life and 19% in the second. In general, we found that sensory and motor regions have maturational trajectories that are different from regions involved with higher order integrative functions, a pattern similar to that described in older children and adolescents in which sensorimotor regions matured through cortical thinning before association areas (Gogtay et al. 2004). In the first 2 years of life, and especially in the first, sensory and motor regions are among the slowest growing regions. These include primary visual processing (calcarine and cuneus), auditory cortex (superior temporal and Heschl gyrus), somatosensory (postcentral gyrus), and motor (precentral, Rolandic, and paracentral lobule) regions. One explanation for the slow early postnatal growth of these regions is more rapid maturation of these regions in the prenatal and early postnatal period before the infant scan (average age 25.5 ± 10.8 days). If so, this is evidence that regions first to initially grow and mature prior to and after birth are the same regions that also mature through thinning first during later childhood development.

Synapse density is much higher after birth in auditory and calcarine cortex compared with prefrontal cortex, and peaks in these sensory regions well before prefrontal cortex (Huttenlocher and Dabholkar 1997). Glucose utilization is also high in the sensorimotor cortex in infants 5 weeks of age and younger, while increasing in frontal and other areas of association cortex by 8 months of age (Chugani and Phelps 1986). Motor, somatosensory, and auditory systems function prior to birth, and the newborn can process information in all sensory modalities, including vision (Kagan and Herschkowitz 2005; Sanes and Bao 2009; Bourne 2010). Higher-order functions such as visual-spatial working memory (Pelphrey et al. 2004) and language-specific speech perception (Kuhl 2004) develop later in the first year of life.

Regions with faster volume increases in the first year include the inferior frontal gyrus and angular gyrus, cortical regions involved with language (Shalom and Poeppel 2008). It is interesting that one of the most rapidly growing regions is the insula, which is involved with a variety of functions, including awareness of interoceptive or visceral sensations, pain, body movement, emotions, vocalizations, and perhaps even consciousness (Augustine 1996; Nagai et al. 2007; Craig 2009). Other faster growing regions are the fusiform gyrus, involved with face recognition and color processing (Bartels and Zeki 2000; Kanwisher and Yovel 2006) and the inferior temporal

**Table 1**

Cortical gray matter volumes and growth rates

| Region | Year 0 Volume ($mm^3$) LS Mean (SE) | Year 1 Volume ($mm^3$) LS Mean (SE) | Year 2 Volume ($mm^3$) LS Mean (SE) | Year 0–1 % Change* | Year 1–2 % Change* | Year 0–2 % Change* |
|---|---|---|---|---|---|---|
| Total cortical GM | 217474.4 (3842.4) | 451625.3 (3842.4) | 537138.4 (3842.4) | 107.7 | 18.9 | 147.0 |
| Central region | | | | | | |
| Precentral_L | 3683.6 (112.0) | 7622.7 (112.0) | 8746.2 (112.0) | 106.9 | 14.7 | 137.4 |
| Precentral_R | 3810.9 (110.1) | 7490.2 (110.1) | 8705.2 (110.1) | 96.6 | 16.2 | 128.4 |
| Postcentral_L | 4831.6 (135.4) | 8052.4 (135.4) | 9243.1 (135.4) | 66.7 | 14.8 | 91.3 |
| Postcentral_R | 4660.8 (141.4) | 7552.4 (141.4) | 8664.1 (141.4) | 62.0 | 14.7 | 85.9 |
| Rolandic_Oper_L | 1671.0 (54.1) | 3302.0 (54.1) | 3726.2 (54.1) | 97.6 | 12.8 | 123.0 |
| Rolandic_Oper_R | 2023.1 (60.3) | 4001.8 (60.3) | 4592.5 (60.3) | 97.8 | 14.8 | 127.0 |
| Frontal lobe | | | | | | |
| Lateral surface | | | | | | |
| Frontal_Sup_L | 3471.9 (122.7) | 7318.0 (122.7) | 8918.2 (122.7) | 110.8 | 21.9 | 156.9 |
| Frontal_Sup_R | 3950.8 (136.0) | 8103.3 (136.0) | 9958.9 (136.0) | 105.1 | 22.9 | 152.1 |
| Frontal_Mid_L | 6835.0 (202.9) | 13770.9 (202.9) | 16760.8 (202.9) | 101.5 | 21.7 | 145.2 |
| Frontal_Mid_R | 7005.0 (205.8) | 13580.0 (205.8) | 16618.1 (205.8) | 93.9 | 22.4 | 137.2 |
| Frontal_Inf_Oper_L | 1154.3 (65.8) | 2732.6 (65.8) | 3197.7 (65.8) | 136.7 | 17.0 | 177.0 |
| Frontal_Inf_Oper_R | 1718.8 (72.3) | 3881.2 (72.3) | 4665.6 (72.3) | 125.8 | 20.2 | 171.4 |
| Frontal_Inf_Tri_L | 3285.5 (127.2) | 6626.5 (127.2) | 7954.2 (127.2) | 101.7 | 20.0 | 142.1 |
| Frontal_Inf_Tri_R | 2675.1 (93.2) | 4954.7 (93.2) | 5941.7 (93.2) | 85.2 | 19.9 | 122.1 |
| Medial surface | | | | | | |
| Frontal_Sup_Medial_L | 3513.8 (128.9) | 7007.3 (128.9) | 8584.9 (128.9) | 99.4 | 22.5 | 144.3 |
| Frontal_Sup_Medial_R | 2592.4 (92.1) | 5165.5 (92.1) | 6420.6 (92.1) | 99.3 | 24.3 | 147.7 |
| Supp_Motor_Area_L | 2357.6 (96.7) | 4978.8 (96.7) | 5996.3 (96.7) | 111.2 | 20.4 | 154.3 |
| Supp_Motor_Area_R | 2479.4 (87.2) | 5050.8 (87.2) | 6037.6 (87.2) | 103.7 | 19.5 | 143.5 |
| Paracentral_Lobule_L | 1125.9 (42.3) | 2011.2 (42.3) | 2218.9 (42.3) | 78.6 | 10.3 | 97.1 |
| Paracentral_Lobule_R | 701.6 (27.8) | 1241.0 (27.8) | 1410.2 (27.8) | 76.9 | 13.6 | 101.0 |
| Orbital surface | | | | | | |
| Frontal_Sup_Orb_L | 1031.6 (31.4) | 2450.12 (31.4) | 2821.83 (31.4) | 137.5 | 15.2 | 173.5 |
| Frontal_Sup_Orb_R | 1226.0 (38.9) | 2889.32 (38.9) | 3328.87 (38.9) | 135.7 | 15.2 | 171.5 |
| Frontal_Med_Orb_L | 1009.2 (35.8) | 2005.66 (35.8) | 2433.25 (35.8) | 98.7 | 21.3 | 141.1 |
| Frontal_Med_Orb_R | 1439.2 (52.7) | 2845.38 (52.7) | 3452.48 (52.7) | 97.7 | 21.3 | 139.9 |
| Frontal_Mid_Orb_L | 1121.1 (41.3) | 2342.61 (41.3) | 2816.35 (41.3) | 108.9 | 20.2 | 151.2 |
| Frontal_Mid_Orb_R | 1475.6 (62.0) | 2903.87 (62.0) | 3549.54 (62.0) | 96.8 | 22.2 | 140.5 |
| Frontal_Inf_Orb_L | 2592.8 (88.6) | 5583.65 (88.6) | 6692.45 (88.6) | 115.4 | 19.9 | 158.1 |
| Frontal_Inf_Orb_R | 2723.5 (87.4) | 5553.79 (87.4) | 6688.07 (87.4) | 103.9 | 20.4 | 145.6 |
| Rectus_L | 1284.6 (46.3) | 2760.90 (46.3) | 3135.39 (46.3) | 114.9 | 13.6 | 144.1 |
| Rectus_R | 1164.6 (35.4) | 2504.36 (35.4) | 2884.17 (35.4) | 115.0 | 15.2 | 147.7 |
| Olfactory_L | 617.1 (21.0) | 1298.61 (21.0) | 1518.69 (21.0) | 110.4 | 16.9 | 146.1 |
| Olfactory_R | 605.9 (19.1) | 1217.51 (19.1) | 1420.46 (19.1) | 100.9 | 16.7 | 134.4 |
| Temporal lobe | | | | | | |
| Temporal_Sup_L | 4647.4 (128.0) | 8639.4 (128.0) | 10366.4 (128.0) | 85.9 | 20.0 | 123.1 |
| Temporal_Sup_R | 5111.8 (120.4) | 9668.0 (120.4) | 11408.3 (120.4) | 89.1 | 18.0 | 123.2 |
| Heschl_L | 553.5 (18.6) | 952.6 (18.6) | 1098.7 (18.6) | 72.1 | 15.3 | 98.5 |
| Heschl_R | 515.7 (19.2) | 857.6 (19.2) | 993.9 (19.2) | 66.3 | 15.9 | 92.7 |
| Temporal_Mid_L | 7406.6 (249.5) | 16524.9 (249.5) | 19510.1 (249.5) | 123.1 | 18.1 | 163.4 |
| Temporal_Mid_R | 7918.0 (218.1) | 17582.3 (218.1) | 20603.4 (218.1) | 122.1 | 17.2 | 160.2 |
| Temporal_Inf_L | 3671.5 (136.9) | 9294.9 (136.9) | 11170.0 (136.9) | 153.2 | 20.2 | 204.2 |
| Temporal_Inf_R | 4805.7 (175.7) | 11874.2 (175.7) | 14167.9 (175.73) | 147.1 | 19.3 | 194.8 |
| Temporal_Pole_Sup_L | 1585.4 (50.6) | 3387.0 (50.6) | 4123.8 (50.56) | 113.6 | 21.8 | 160.1 |
| Temporal_Pole_Sup_R | 1820.0 (53.9) | 3665.5 (53.9) | 4513.5 (53.9) | 101.4 | 23.1 | 148.0 |
| Temporal_Pole_Mid_L | 787.4 (37.4) | 1949.0 (37.4) | 2470.6 (37.4) | 147.5 | 26.8 | 213.8 |
| Temporal_Pole_Mid_R | 1153.9 (53.5) | 2580.7 (53.5) | 3222.2 (53.5) | 123.6 | 24.9 | 179.2 |
| Insula | | | | | | |
| Insula_L | 2904.7 (80.4) | 6976.9 (80.4) | 8199.4 (80.4) | 140.2 | 17.5 | 182.3 |
| Insula_R | 2621.9 (72.7) | 6664.5 (72.7) | 7746.9 (72.7) | 154.2 | 16.2 | 195.5 |
| Cingulum | | | | | | |
| Cingulum_Ant_L | 2676.6 (91.7) | 5667.2 (91.7) | 6734.4 (91.7) | 111.7 | 18.8 | 151.6 |
| Cingulum_Ant_R | 2418.1 (89.3) | 5264.0 (89.3) | 6213.1 (89.3) | 117.7 | 18.0 | 156.9 |
| Cingulum_Mid_L | 3527.2 (122.9) | 7867.3 (122.8) | 9330.9 (122.8) | 123.0 | 18.6 | 164.5 |
| Cingulum_Mid_R | 3654.2 (120.8) | 8490.2 (120.8) | 10101.5 (120.8) | 132.3 | 19.0 | 176.4 |
| Cingulum_Post_L | 606.1 (27.2) | 1335.9 (27.2) | 1538.8 (27.2) | 120.4 | 15.2 | 153.9 |
| Cingulum_Post_R | 365.4 (17.1) | 733.3 (17.1) | 842.5 (17.1) | 100.7 | 14.9 | 130.6 |
| Parietal lobe | | | | | | |
| Parietal_Sup_L | 2184.1 (89.7) | 4256.6 (89.7) | 5114.9 (89.7) | 94.9 | 20.2 | 134.2 |
| Parietal_Sup_R | 2613.4 (114.7) | 4883.5 (114.7) | 5941.3 (114.7) | 86.9 | 21.7 | 127.3 |
| Parietal_Inf_L | 4008.6 (144.0) | 8367.1 (144.0) | 10522.3 (144.0) | 108.7 | 25.8 | 162.5 |
| Parietal_Inf_R | 2738.2 (131.4) | 5763.7 (131.4) | 7198.0 (131.4) | 110.5 | 24.9 | 162.9 |
| Angular_L | 2552.0 (149.6) | 5858.9 (149.6) | 7280.0 (149.6) | 129.6 | 24.3 | 185.3 |
| Angular_R | 3537.0 (177.9) | 7903.6 (177.9) | 9867.4 (177.9) | 123.5 | 24.8 | 179.0 |
| SupraMarginal_L | 1828.0 (84.6) | 3633.0 (84.6) | 4568.3 (84.6) | 98.7 | 25.7 | 149.9 |
| SupraMarginal_R | 3065.9 (153.7) | 5984.1 (153.7) | 7669.7 (153.7) | 95.2 | 28.2 | 150.2 |
| Precuneus_L | 6671.0 (183.0) | 13277.8 (183.0) | 16037.6 (183.0) | 99.0 | 20.8 | 140.4 |
| Precuneus_R | 5259.7 (152.2) | 11243.3 (152.2) | 13455.5 (152.3) | 113.8 | 19.7 | 155.8 |
| Occipital lobe | | | | | | |
| Occipital_Sup_L | 1915.0 (79.8) | 3856.3 (79.8) | 4432.3 (79.8) | 101.4 | 14.9 | 131.4 |
| Occipital_Sup_R | 1724.8 (65.0) | 3460.0 (65.0) | 4030.4 (65.0) | 100.6 | 16.5 | 133.7 |
| Occipital_Mid_L | 4636.4 (170.5) | 10334.3 (170.5) | 11677.9 (170.5) | 122.9 | 13.0 | 151.9 |

**Table 1**
Continued

| Region | Year 0 Volume ($mm^3$) LS Mean (SE) | Year 1 Volume ($mm^3$) LS Mean (SE) | Year 2 Volume ($mm^3$) LS Mean (SE) | Year 0–1 % Change* | Year 1–2 % Change* | Year 0–2 % Change* |
|---|---|---|---|---|---|---|
| Occipital_Mid_R | 3531.6 (130.1) | 7634.3 (130.1) | 8553.2 (130.1) | 116.2 | 12.0 | 142.2 |
| Occipital_Inf_L | 1241.1 (56.3) | 2731.0 (56.3) | 3122.5 (56.3) | 120.1 | 14.3 | 151.6 |
| Occipital_Inf_R | 1328.2 (59.7) | 2960.4 (59.7) | 3242.9 (59.7) | 122.9 | 9.5 | 144.2 |
| Cuneus_L | 3343.8 (114.7) | 6029.1 (114.7) | 7056.0 (114.7) | 80.3 | 17.0 | 111.0 |
| Cuneus_R | 2946.3 (106.1) | 5408.2 (106.1) | 6423.4 (106.1) | 83.6 | 18.8 | 118.0 |
| Calcarine_L | 4549.5 (149.1) | 7980.5 (149.1) | 8934.3 (149.1) | 75.4 | 12.0 | 96.4 |
| Calcarine_R | 3560.1 (133.9) | 6432.1 (133.9) | 7108.0 (133.9) | 80.7 | 10.5 | 99.7 |
| Lingual_L | 3073.1 (93.9) | 6467.0 (93.9) | 7564.4 (93.9) | 110.4 | 17.0 | 146.2 |
| Lingual_R | 3020.4 (87.8) | 6122.1 (87.8) | 7162.6 (87.8) | 102.7 | 17.0 | 137.1 |
| Fusiform_L | 3144.5 (99.2) | 7726.4 (99.2) | 9409.1 (99.2) | 145.7 | 21.8 | 199.2 |
| Fusiform_R | 3084.7 (94.7) | 7601.5 (94.7) | 9181.3 (94.7) | 146.4 | 20.8 | 197.6 |

Note: light gray highlight: lowest 25% of volume change and dark gray highlight: highest 25% of volume change. L, left; R, right; Oper, operculum; Sup, superior; Mid, middle; Inf, inferior; Tri, Trigone.
*Significant change in volume for each region for each time period, $P < 0.001$.

**Table 2**
Subcortical gray matter and lateral ventricle volumes and growth rates

| Region | Year 0 Volume ($mm^3$) LS mean (SE) | Year 1 Volume ($mm^3$) LS means (SE) | Year 2 Volume ($mm^3$) LS mean (SE) | Year 0–1 % Change* | Year 1–2 % Change* | Year 0–2 % Change* |
|---|---|---|---|---|---|---|
| Lateral_vent | 4738.6 (122.2) | 9798.1 (122.2) | 11613.4 (122.2) | 106.8 | 18.5 | 145.1 |
| Amygdala_L | 541.9 (12.5) | 1113.6 (12.5) | 1220.9 (12.5) | 105.5 | 9.6 | 125.3 |
| Amygdala_R | 515.4 (12.5) | 1057.0 (12.5) | 1172.2 (12.5) | 105.1 | 10.9 | 127.5 |
| Hippocampus_L | 1466.0 (34.9) | 2671.5 (34.9) | 3165.0 (34.9) | 82.2 | 18.5 | 115.9 |
| Hippocampus_R | 1433.6 (28.6) | 2667.8 (28.6) | 3086.5 (28.6) | 86.1 | 15.7 | 115.3 |
| Thalamus_L | 2426.6 (48.2) | 4980.4 (48.2) | 5677.5 (48.2) | 105.2 | 14.0 | 134.0 |
| Thalamus_R | 2396.4 (48.4) | 4915.1 (48.4) | 5567.0 (48.4) | 105.1 | 13.3 | 132.3 |
| Caudate_L | 1998.4 (52.8) | 4117.7 (52.8) | 4732.9 (52.8) | 106.1 | 14.9 | 136.8 |
| Caudate_R | 2125.3 (51.3) | 4399.4 (51.3) | 5065.8 (51.3) | 107.0 | 15.1 | 138.4 |
| Putamen_L | 2423.6 (40.9) | 4964.0 (40.9) | 5336.2 (40.9) | 104.8 | 7.5 | 120.2 |
| Putamen_R | 2506.5 (43.8) | 5143.5 (43.8) | 5587.2 (43.8) | 105.2 | 8.6 | 122.9 |
| Pallidum_L | 593.9 (16.1) | 1227.2 (16.1) | 1454.1 (16.1) | 106.7 | 18.5 | 144.8 |
| Pallidum_R | 623.3 (17.3) | 1294.6 (17.3) | 1535.4 (17.3) | 107.7 | 18.6 | 146.3 |

Note: L, left; R, right.
*Significant change in volume for each region for each time period, $P < 0.001$.

gyrus, involved with higher-order visual processing, including shape and faces (Denys et al. 2004; Sabatinelli et al. 2011).

In the second year of life, regions of the frontal and parietal cortex have relatively greater volume increases than other cortical areas, consistent with the later maturation of these regions as discussed above (Chugani and Phelps 1986; Huttenlocher and Dabholkar 1997). This pattern of structural maturation is also consistent with more recent studies of cortical network maturation. In infants, resting state functional networks, assessed with functional MRI, are present in sensorimotor regions (Fransson et al. 2007; Lin et al. 2008), with cortical network hubs present in motor, sensory, auditory, and visual primary cortex (Fransson et al. 2011). In contrast, the default network, which involves parietal and prefrontal cortex, does not fully develop until 2 years of age (Gao et al. 2009).

The rapid gray matter growth rates observed in our study are consistent with the rapid elaboration of synapses in this time period (Huttenlocher and Dabholkar 1997; Glantz et al. 2007; Webster et al. 2011). Qualitative golgi studies indicate rapid increase in dendritic complexity of cortical neurons in the first 2 years of life (Conel 1939–1967). More recent studies find rapid development of prefrontal layer 3C pyramidal neuron spines in the first 2 years of life (Petanjek et al. 2011). The total number of basal dendritic segments increased after birth to adult levels by 1 month of age, and the total dendrite length increased 3 times in the first 2.5 months after birth, remained "dormant" until 16 months and then increased again until 2.5 years (Petanjek et al. 2008). In layer 5 pyramidal neurons, no new dendritic segments were elaborated after birth, and adult values of dendritic length were attained by 12–15 months of age (Petanjek et al. 2008). The growth of gray matter volume then appears to be driven mainly by the elongation of existing dendrites and the development of new synapses. Development of gray matter volume is also driven by growth of glial and vascular elements of the neuropil.

The relative patterns of cortical gray matter growth observed in this study are relevant for understanding abnormalities of cortical development observed in neurodevelopmental and neuropsychiatric disorders. Autism is associated with increased gray matter volume that arises after birth and before 2 years of age (Hazlett et al. 2005; Schumann et al. 2010; Hazlett et al. 2011). The first year of postnatal cortical gray matter development is much more rapid than the second and suggests that gray matter overgrowth in autism may be more likely to arise in the first year, during this time of rapid development. We recently found increased cortical gray matter volumes in neonate males at genetic high risk for schizophrenia (Gilmore, Kang, et al. 2010) suggesting that the smaller gray matter volumes observed in schizophrenia develop after birth, perhaps

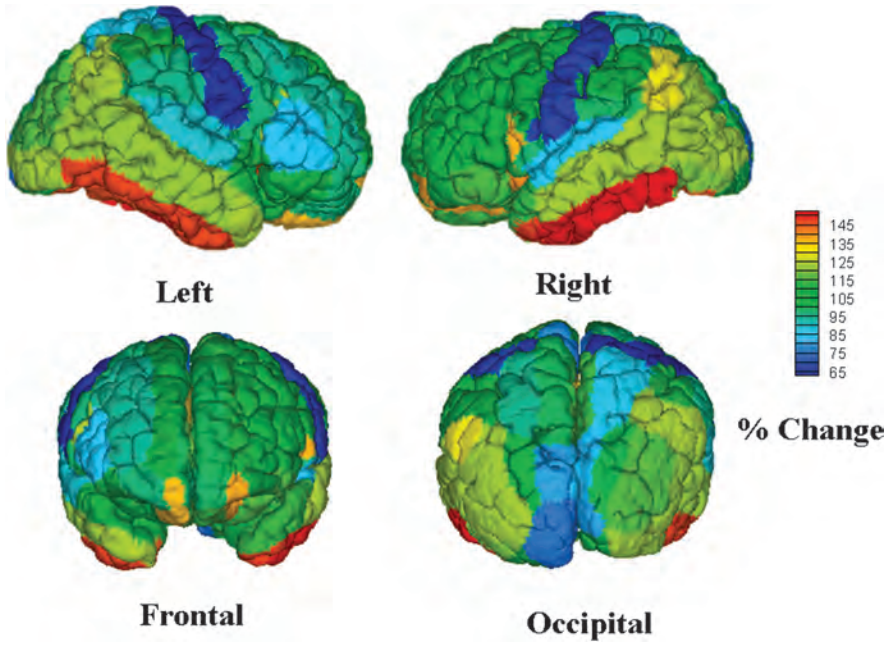


**Figure 2.** Regional growth rates of cortical gray matter volume from birth to 1 year of age.

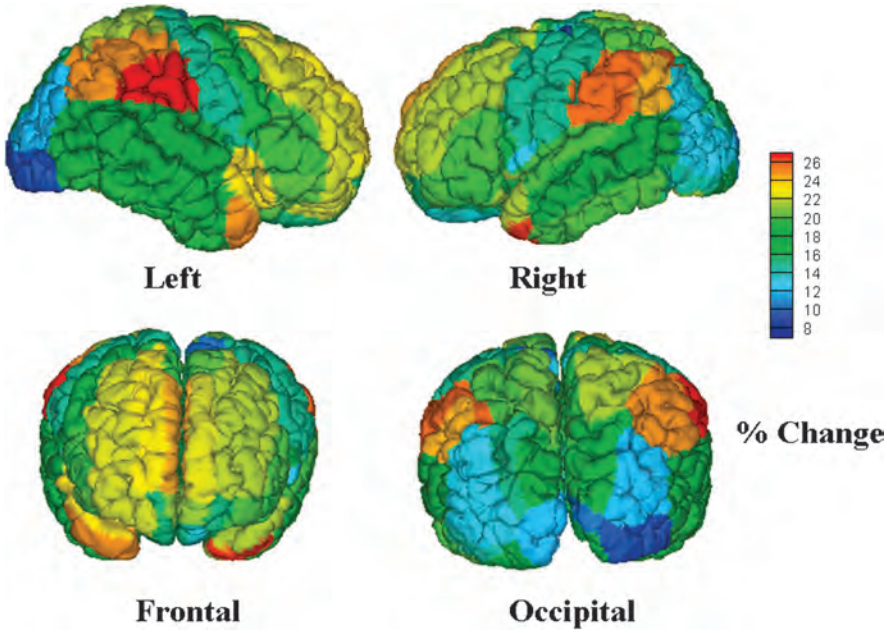


**Figure 3.** Regional growth rates of cortical gray matter volume from 1 to 2 years.

due to abnormalities in this period of rapid gray matter growth in the first 2 years after birth. Finally, cortical thinning has been observed in children at increased familial risk for major depression, indicative of alterations of cortical development in early childhood (Peterson et al. 2009).

There is ample evidence that activity and experience shapes formation and elimination of synapses in the developing brain (Hua and Smith 2004), though the relative contribution of genetic and environmental factors to human gray matter development in this period of rapid growth and development is not clear. Studies in adults and older children find high heritability of gray matter volumes of about 0.82 (Baare et al. 2001; Wallace et al. 2006). We found a heritability of 0.56 for gray matter volume in neonates, indicating that heritability increases with age in early childhood (Gilmore, Schmitt, et al. 2010). Twin studies in young children are needed to confirm this.

To our knowledge, this study is one of the first to provide information about the development of subcortical structures from birth to 2 years of age. In older children, there is heterogeneity of developmental trajectories of subcortical structures (Giedd et al. 1996; Østby et al., 2009). An early study of hippocampal volume from 3 weeks to 14 years of age found a rapid increase in volume in the first 2 years of life,

consistent with our results (Utsunomiya et al. 1999). We studied caudate and hippocampal growth from 1 to 2 years in our previous cross-sectional study (Knickmeyer et al. 2008), and the results of that study are similar to this one. The longitudinal atlas allows the study of these and other subcortical structures from birth. In the first year, the hippocampus tended to have smaller volume growth (82–86%) compared with the other subcortical structures, which had a similar range of volume increase (104–107%). In the second year of life, the hippocampus was one of the faster growing structures, perhaps consistent with the acquisition of episodic memory (Tustin and Hayne 2010), as well as spatial working memory and path integration abilities (McNaughton et al. 2006, Wolbers et al. 2007) as the child becomes more mobile, in the second year of life.

Overall, our cortical gray matter findings are consistent with our previous cross-sectional study (Knickmeyer et al 2008). In both studies, we found large increases in overall gray matter volumes in the first year of life, with smaller but significant growth in the second. There was a difference in the magnitude of growth in the first year of life between studies, while the rates of growth in the second year are very similar. The differences in the first year growth rates may reflect the improved ability of longitudinal study designs to detect differences over time, though differences in tissue segmentation methodologies may also contribute. In our earlier cross-sectional study, we found that there was a small decrease of lateral ventricle volume in the second year of life (Knickmeyer et al 2008); though in this study, we observed a small but significant increase in lateral ventricle volumes, highlighting the importance of longitudinal studies for tracking developmental trajectories.

In summary, we found overall rapid growth of overall cortical gray matter volume and clear regional differences in volume growth in the first 2 years of life using a novel longitudinal registration/parcellation. These regional differences are consistent with regional differences in synapse development as well as with the functional and cognitive development that these regions support. The first 2 years of life are a period of robust gray matter growth and likely represent a critical period of development and vulnerability for neurodevelopmental disorders.

## Funding

National Institutes of Health (grant P50 MH064065, HD053000, and MH070890 to J.H.G).

## Notes

*Conflict of Interest* : None declared.

## References

Amaral DG, Schumann CM, Nordahl CW. 2008. Neuroanatomy of autism. Trends Neurosci. 31:137–145.

Augustine JR. 1996. Circuitry and functional aspects of the insular lobe in primates including humans. Brain Res Brain Res Rev. 22:229–244.

Baare WF, Hulshoff Pol HE, Boomsma DI, Posthuma D, de Geus EJ, Schnack HG, van Haren NE, van Oel CJ, Kahn RS. 2001. Quantitative genetic modeling of variation in human brain morphology. Cereb Cortex. 11:816–824.

Bartels A, Zeki S. 2000. The architecture of the colour centre in the human visual brain: new results and a review. Eur J Neurosci. 12:172–193.

Bourne JA. 2010. Unravelling the development of the visual cortex: implications for plasticity and repair. J Anat. 217:449–468.

Chi JG, Dooling EC, Gilles FH. 1977. Gyral development of the human brain. Ann Neurol. 1:86–93.

Chugani HT, Phelps ME. 1986. Maturational changes in cerebral function in infants by 18FDG positron emission tomography. Science. 231:840–843.

Conel JL. 1939–1967. The postnatal development of the human cortex. Vols. 1–6. Cambridge (MA): Harvard University Press.

Courchesne E, Pierce K, Schumann CM, Redclay E, Buckwalter JA, Kennedy DP, Morgan J. 2007. Mapping early brain development in autism. Neuron. 56:399–413.

Craig AD. 2009. How do you feel–now? The anterior insula and human awareness. Nat Rev Neurosci. 10:59–70.

Denys K, Vanduffel W, Fize D, Nelissen K, Peuskens H, Van Essen D, Orban GA. 2004. The processing of visual shape in the cerebral cortex of human and nonhuman primates: a functional magnetic resonance imaging study. J Neurosci. 24:2551–2565.

Dice LR. 1945. Measures of the amount of ecologic association between species. Ecology. 26:297–302.

Fransson P, Aden U, Blennow M, Lagercrantz H. 2011. The functional architecture of the infant brain as revealed by resting-state FMRI. Cereb Cortex. 21:145–154.

Fransson P, Skiold B, Horsch S, Nordell A, Blennow M, Lagercrantz H, Aden U. 2007. Resting-state networks in the infant brain. Proc Natl Acad Sci U S A. 104:15531–15536.

Gao W, Zhu H, Giovanello KS, Smith JK, Shen D, Gilmore JH, Lin W. 2009. Evidence on the emergence of the brain's default network from 2-week-old to 2-year-old healthy pediatric subjects. Proc Natl Acad Sci U S A. 106:6790–6795.

Giedd JN, Blumenthal J, Jeffries NO, Castellanos FX, Liu H, Zijdenbos A, Paus T, Evans AC, Rapoport JL. 1999. Brain development during childhood and adolescence: a longitudinal MRI study. Nat Neurosci. 2:861–863.

Giedd JN, Snell JW, Lange N, Rajapakse JC, Casey BJ, Kozuch PL, Vaituzis AC, Vauss YC, Hamburger SD, Kaysen D, et al. 1996. Quantitative magnetic resonance imaging of human brain development: ages 4–18. Cereb Cortex. 6:551–560.

Gilmore JH, Kang C, Evans DD, Wolfe HM, Smith KS, Lieberman JA, Lin W, Hamer RM, Styner M, Gerig G. 2010. Prenatal and neonatal brain structure and white matter maturation in children at high risk for schizophrenia. Am J Psychiatry. 167:1083–1091.

Gilmore JH, Lin W, Prastawa MW, Looney CB, Vetsa YSK, Knickmeyer RC, Evans DD, Smith JK, Hamer RM, Lieberman JA, et al. 2007. Regional gray matter growth, sexual dimorphism and cerebral asymmetry in the neonatal brain. J Neurosci. 27:1255–1260.

Gilmore JH, Schmitt JE, Knickmeyer RA, Smith JK, Lin W, Styner M, Gerig G, Neale MC. 2010. Genetic and environmental contributions to neonatal brain structure: a twin study. Hum Brain Mapp. 31:1174–1182.

Glantz LA, Gilmore JH, Hamer RM, Lieberman JA, Jarskog LF. 2007. Synaptophysin and PSD-95 in the human prefrontal cortex from mid-gestation into early adulthood. Neuroscience. 149:582–91.

Gogtay N, Giedd JN, Lusk L, Hayashi KM, Greenstein D, Vaituzis AC, Nugent TF, Herman DH, Clasen LS, Toga AW, et al. 2004. Dynamic mapping of human cortical development during childhood through early adulthood. Proc Natl Acad Sci U S A. 101:8174–8179.

Hazlett HC, Poe MD, Gerig G, Smith RG, Provenzale J, Ross A, Gilmore JH, Piven J. 2005. An MRI and head circumference study of brain size in autism: birth through age two years. Arch Gen Psychiatry. 62:1366–1376.

Hazlett HC, Poe MD, Gerig G, Styner M, Chappell C, Smith RG, Vachet C, Piven J. 2011. Early brain overgrowth in autism associated with an increase in cortical surface area before age 2 years. Arch Gen Psychiatry. 68:467–476.

Hill J, Dierker D, Neil J, Inder T, Knutsen A, Harwell J, Coalson T, Van Essen D. 2010. A surfaced-based analysis of hemispheric asymmetries and folding of the cerebral cortex in term-born human infants. J Neurosci. 30:2268–2276.

Hua JY, Smith SJ. 2004. Neural activity and the dynamics of central nervous system development. Nat Neurosci. 7:327–332.

Huttenlocher PR, Dabholkar AS. 1997. Regional differences in synaptogenesis in human cerebral cortex. J Comp Neurol. 387:167–178.

Kagan J, Herschkowitz N. 2005. A young mind in a growing brain. Mahwah (NJ): Lawrence Erlbaum Associates.

Kanwisher N, Yovel G. 2006. The fusiform face area: a cortical region specialized for the perception of faces. Philos Trans R Soc Lond B Biol Sci. 361:2109–2128.
Knickmeyer RC, Gouttard S, Lin W, Evans DD, Wilber K, Smith JK, Kang C, Hamer RM, Gerig G, Gilmore JH. 2008. A structural MRI study of human brain development from birth to age 2. J Neurosci. 28:12176–12182.
Knickmeyer RC, Kang C, Woolson S, Smith JK, Hamer RM, Lin W, Gerig G, Styner M, Gilmore JH. 2011. Twin-singleton differences in neonatal brain structure. Twin Res Hum Genet. 14:268–76.
Kuhl PK. 2004. Early language acquisition: cracking the speech code. Nat Rev Neurosci. 5:831–843.
Lin W, Zhu Q, Gao W, Chen Y, Toh CH, Styner M, Gerig G, Smith JK, Biswal B, Gilmore JH. 2008. Functional connectivity MR imaging reveals cortical functional connectivity in the developing brain. AJNR Am J Neuroradiol. 29:1883–1889.
Looney CB, Smith JK, Fagan LH, Wolfe HM, Chescheir NC, Hamer RM, Gilmore JH. 2007. Intracranial hemorrhage in asymptomatic neonates: prevalence on MR images and relationship to obstetric and neonatal risk factors. Radiology. 242:535–541.
Matsuzawa J, Matsui M, Konishi T, Noguchi K, Gur RC, Bilker W, Miyawaki T. 2001. Age-related changes of brain gray and white matter in healthy infants and children. Cereb Cortex. 11:335–342.
McNaughton BL, Battaglia FP, Jensen O, Moser EI, Moser MB. 2006. Path integration and the neural basis of the cognitive map. Nat Rev Neurosci. 7:663–678.
Mullen, EM. 1995. Mullen scales of early learning. AGS ed. Circle Pines (MN): American Guidance Service Inc.
Nagai M, Kishi K, Kato S. 2007. Insular cortex and neuropsychiatric disorders: a review of recent literature. Eur Psychiatry. 22:387–394.
Østby Y, Tamnes CK, Fjell AM, Westlye LT, Due-Tønnessen P, Walhvod KB. 2009. Heterogeneity in subcortical brain development: a structural magnetic resonance imaging study of brain maturation from 8 to 30 years. J Neurosci. 29:11772–11782.
Pelphrey KA, Reznick JS, Goldman BD, Sasson N, Morrow J, Donahoe A, Hodgson K. 2004. Development of visualspatial short-term memory in the second half of the first year of life. Dev Psychol. 40:836–851.
Petanjek Z, Judas M, Kostovic I, Uylings HBM. 2008. Lifespan alterations of basal dendritic trees of pyramidal neurons in the human prefrontal cortex: a layer-specific pattern. Cereb Cortex. 18: 915–929.
Petanjek Z, Judas M, Simic G, Rasin MR, Uylings HB, Rakic P, Kostovic I. 2011. Extraordinary neoteny of synaptic spines in the human prefrontal cortex. Proc Natl Acad Sci U S A. 108:13281–13286.
Peterson BS, Warner V, Bansal R, Zhu H, Hao X, Liu J, Durkin K, Adams PB, Wickramaratne P, Weissman MM. 2009. Cortical thinning in persons at increased familial risk for major depression. Proc Natl Acad Sci U S A. 106:6273–6278.
Pham DL, Prince JL. 1999. An adaptive fuzzy C-means algorithm for image segmentation in the presence of intensity inhomogeneities. Pattern Recognit Lett. 20:57–68.
Sabatinelli D, Fortune EE, Li Q, Siddiqui A, Krafft C, Oliver WT, Beck S, Jeffries J. 2011. Emotional perception: meta-analyses of face and natural scene processing. Neuroimage. 54:2524–2533.
Sanes DH, Bao S. 2009. Tuning up the developing auditory CNS. Curr Opin Neurobiol. 19:188–199.
Schumann CM, Bloss CS, Barnes CC, Wideman GM, Carper RA, Akshoomoff N, Pierce K, Hagler D, Schork N, Lord C, et al. 2010. Longitudinal magnetic resonance imaging study of cortical development through early childhood in autism. J Neurosci. 30: 4419–4427.
Shalom DB, Poeppel D. 2008. Functional anatomic models of language: assembling the pieces. Neuroscientist. 14:119–127.
Shaw P, Kabani NJ, Lerch JP, Eckstrand K, Lenroot R, Gogtay N, Greenstein D, Clasen L, Evans A, Rapoport JL, et al. 2008. Neurodevelopmental trajectories of the human cerebral cortex. J Neurosci. 28:3586–3594.
Shen D, Davatzikos C. 2002. HAMMER: hierarchical attribute matching mechanism for elastic registration. IEEE Trans Med Imaging. 21: 1421–1439.
Shi F, Fan Y, Tang S, Gilmore JH, Lin W, Shen D. 2010. Neonatal brain image segmentation in longitudinal studies. Neuroimage. 49:391–400.
Shi F, Yap P-T, Wu G, Jia H, Gilmore JH, Lin W, Shen D. 2011. Infant brain atlases from neonates to 1- and 2-year-olds. PLoS One. 6:e18746.
Sowell ER, Peterson BS, Thompson PM, Welcome SE, Henkenius AL, Toga AW. 2003. Mapping cortical change across the human life span. Nat Neurosci. 6:309–315.
Sowell ER, Thompson PM, Holmes CJ, Jernigan TL, Toga AW. 1999. In vivo evidence for post-adolescent brain maturation in frontal and striatal regions. Nat Neurosci. 2:859–861.
Sowell ER, Thompson PM, Leonard CM, Welcome SE, Kan E, Toga AW. 2004. Longitudinal mapping of cortical thickness and brain growth in normal children. J Neurosci. 24:8223–8231.
Tustin K, Hayne H. 2010. Defining the boundary: age related changes in childhood amnesia. Dev Psychol. 46:1049–1061.
Tzourio-Mazoyer N, Landeau B, Papathanassiou D, Crivello F, Etard O, Delicrox N, Mazoyer B, Joliet M. 2002. Automated anatomical labeling of activations in SPM using amacroscopic anatomical parcellation of the MNI MRI single-subject brain. Neuroimage. 15:273–289.
Utsunomiya H, Takano K, Okazaki M, Mitsudome A. 1999. Development of the temporal lobe in infants and children: analysis by MR-based volumetry. AJNR Am J Neuroradiol. 20:717–723.
Wallace GL, Schmitt JE, Lenroot R, Viding E, Ordaz S, Rosenthal MA, Molloy EA, Clasen LS, Kendler KS, Neale MC, et al. 2006. A pediatric twin study of brain morphometry. J Child Psychol Psychiatry. 47:987–993.
Webster MJ, Elashoff M, Sahnnon Weickert C. 2011. Molecular evidence that cortical synaptic growth predominates during the first decade of life in humans. Int J Dev Neurosci. 29:225–236.
Wolbers T, Wiener JM, Mallot HA, Buchel C. 2007. Differential recruitment of the hippocampus, medial prefrontal cortex, and the human motion complex during path integration in humans. J Neurosci. 27:9408–9416.
Yakovlev PI, Lecours AR. 1967. The myelogenetic cycles of regional maturation in the brain. In: Minkowski A, editor. Regional development of the brain in early life. London: Blackwell. p. 3–70.